QPSK wavelength multicasting based on four-wave mixing in semiconductor optical amplifier

Jun Qin (秦 军)[1], Hongxiang Wang (王宏祥)[1], Danshi Wang (王丹石)[1], Min Zhang (张 民)[1], Yuefeng Ji (纪越峰)[1*], and Guo-Wei Lu (吕国伟)[2]

[1]*State Key Laboratory of Information Photonics and Optical Communication, School of Information and Communication Engineering, Beijing University of Posts and Telecommunications, Beijing, China*

[2]*Institute of Innovative Science and Technology, Tokai University, Kanagawa 259-1193, Japan*

[*]*Corresponding author: jyf@bupt.edu.cn*

Received June 4, 2014; accepted July 16, 2014; posted online October 24, 2014

We experimentally demonstrate one-to-five quadrature phase-shift keying (QPSK) wavelength multicasting based on four-wave mixing in bulk semiconductor optical amplifier. The input 25 Gb/s nonreturn-to-zero QPSK signal is successfully multicast to five new wavelengths with all information preserved. All the multicast channels are with a power penalty less than 1.1 dB at a bit error rate (BER) of 10^{-3}. A characterization of the conversion efficiency in terms of pump and signal powers using the BER as figure of merit is also presented, the results indicate that the pump and signal powers should be optimized to eliminate the introduced deleterious nonlinear components.

OCIS codes: 060.0060, 070.4340, 190.4380.
doi: 10.3788/COL201412.110601.

In recent years, all optical wavelength division multiplexing (WDM) multicasting which can efficiently deliver a stream of information carried by one input wavelength to a number of different output wavelengths has been regarded as an essential and important functionality in the next generation all optical transparent networks, especially with the emerging of the services such as high-definition TV and migration operations in data centers. Data delivering of streaming media or high-definition TV and data center migration operations are all characterized by delivering the information carried by a channel at certain input wavelength to a number of different output wavelengths, which are just the functionalities of WDM multicasting. By employing the WDM multicasting technology, the network efficiency and throughput will be improved effectively[1], and with an all-optical way, the cost and energy consumption can be reduced significantly compared with the traditional electronic way.

During the past decade, multiple wavelength multicasting schemes have been extensively studied and demonstrated in various nonlinear devices including highly nonlinear fiber[2–6], silicon nanowire[7], and silicon waveguide[8]. But most of these schemes suffer from drawbacks such as high input powers, poor conversion efficiency (CE), and complicated system architecture. And, these works mainly involved with intensity modulated nonreturn-to-zero on-off-keying (NRZ-OOK) signal, return-to-zero (RZ) OOK signal, and differential phase-shift-keying (DPSK) signal. Adams *et al.*[7] discussed the multicasting of 16-ary quadrature amplitude modulation (16QAM) in silicon nanowire. However, a poor system performance was obtained (with a worst case power penalty of about 7.8 dB at the forward error correction (FEC) limit). The principle is not clear about the polarization state of the two pumps (parallel or orthogonal) and the other detailed parameters of the experiment (such as the CE and the optical signal-to-noise ratio (OSNR) of the output channels) are not given. With periodically-poled lithium niobate (PPLN) waveguide, multicasting for 16QAM signal has also been reported in Ref. [9], but with too less number of output multicast wavelengths and suffers poor performance due to the PPLN damage power threshold.

Quadrature phase-shift keying (QPSK) is an attractive data modulation format, by multilevel data encoding, its symbol rate is half the bit rate on the transmission line facilitating the improvement of the spectral efficiency. QPSK has been scheduled for use in the commercial 100 Gb/s Ethernet system, so the multicasting of QPSK signal will have more practical significance. As an obbligato device in optical signal processing, semiconductor optical amplifier (SOA) offers advantages in terms of integration potential, low power consumption, and high CE[10]. Four-wave mixing (FWM) in SOA has been proposed for wavelength multicasting as an efficient way[11]. Contestabile *et al.*[11] demonstrated a scheme for multicasting an input signal to six output wavelengths employing three pumps with different states of polarization. However, the scheme suffers complexity in controlling the polarization state, low signal bit rate, and simply contraposing NRZ signal, and the results cannot be extended to phase modulated signals in a straight forward way[12]. On the other hand, the FWM based on dual-pump in SOA shows advantages in complexity, enhanced conversion

bandwidth[13], and transparency to modulation formats, it is a wise choice for high-order modulation signal multicasting operation. Quantum-dot (QD) SOAs have also attracted interest for wavelength multicasting based on cross-gain modulation[14] for RZ signals, but the schemes are not suitable for phase-modulated signal. Contestabile *et al.*[15,16] showed broadband conversion of QPSK and other modulation formats in QD-SOAs with multipump FWM which can also provide multicast by its working principle. In addition, the wavelength conversion employing QD-SOA yield similar performances using traditional SOA and the severe polarization sensitivity are still issues with QD-SOA[12], Compared with QD-SOA, the mature bulk SOAs may still be the best choice for wavelength multicasting.

Here to the best of our knowledge, for the first time we experimentally demonstrated one-to-five 25 Gb/s NRZ-QPSK wavelength multicasting based on FWM in a bulk SOA device. All the new generated five channels exhibit good OSNR, reach a maximum power penalty of 1.1 dB at a bit error rate (BER) of 10^{-3}. A characterization of the CE in terms of pump and signal powers using the BER as figure of merit was also presented, the results indicated that the pump and signal powers should be optimized to eliminate the introduced deleterious nonlinear components. Except the five multicast QPSK signals, two binary phase-shift keying (BPSK) signals were also successfully obtained because of the phase erasing characteristic of the FWM process.

Figure 1 illustrates the principle of the QPSK wavelength multicasting based on FWM in SOA employing two pumps. As shown in Fig. 1, at the input side of the SOA are three FWM participators including two pump lights at frequencies f_1 and f_2, and a signal light at f_s. Through a WDM these three waves are injected into SOA. Both degenerate FWM (D-FWM) and non-degenerate FWM (ND-FWM) happen inside the SOA and nine new frequencies will be generated[17], as shown in Fig. 1. Each of the generated component through D-FWM and ND-FWM possesses a frequency of $f_{\rm abc} = f_a + f_b - f_c$ ($b \neq c$, a, b, and c select from 1, 2, and s), and a phase of $\varphi_{\rm abc} = \varphi_a + \varphi_b - \varphi_c$ ($b \neq c$, a, b, and c select from 1, 2, and s)[18,19]. When $a = b$, it is D-FWM component, whereas when $a \neq b$ it is ND-FWM component. We can derive the relationship of electrical field (E) and optical phase (φ) for the generated idlers at λ_{A1}–λ_{A5} (λ_{A1} and λ_{A3} are D-FWMs and λ_{A2}, λ_{A4}, and λ_{A5} are ND-FWMs) as

$$E_{A1} \propto A_1^2 A_s^*, \quad \varphi_{A1} = 2\varphi_1 - \varphi_s, \tag{1}$$

$$E_{A2} \propto A_1 A_2 A_s^*, \quad \varphi_{A2} = \varphi_1 + \varphi_2 - \varphi_s, \tag{2}$$

$$E_{A3} \propto A_2^2 A_s^*, \quad \varphi_{A3} = 2\varphi_2 - \varphi_s, \tag{3}$$

$$E_{A4} \propto A_1 A_s A_2^*, \quad \varphi_{A4} = \varphi_1 + \varphi_s - \varphi_2, \tag{4}$$

$$E_{A5} \propto A_2 A_s A_1^*, \quad \varphi_{A5} = \varphi_2 + \varphi_s - \varphi_1, \tag{5}$$

where A_i, $i \in (1, 2, s)$ is the field amplitude of the input lights and * represents the conjugate operation. Since the two pumps at frequencies f_1 and f_2 are not phase modulated (i.e., constant phase), it can be derived from Eqs. (1) to (5) that the original QPSK signal at f_s will be simultaneously transferred to λ_{A1}–λ_{A5} with all information (both amplitude and phase) preserved, therefore one to five (not including the original signal light) QPSK WDM wavelength multicasting will be achieved. At the same time, the electrical field and optical phase of the idlers at λ_{C1}–λ_{C2} satisfy

$$E_{C1} \propto A_s^2 A_2^*, \quad \varphi_{C1} = 2\varphi_s - \varphi_2, \tag{6}$$

$$E_{C2} \propto A_s^2 A_1^*, \quad \varphi_{C2} = 2\varphi_s - \varphi_1. \tag{7}$$

Equations (6) and (7) show that the resultant phase at λ_{C1} and λ_{C2} are doubled with respect to the phase patterns carried in the input signal at λ_s, so when the input is QPSK, BPSK signal will be obtained at λ_{C1} and λ_{C2}[20].

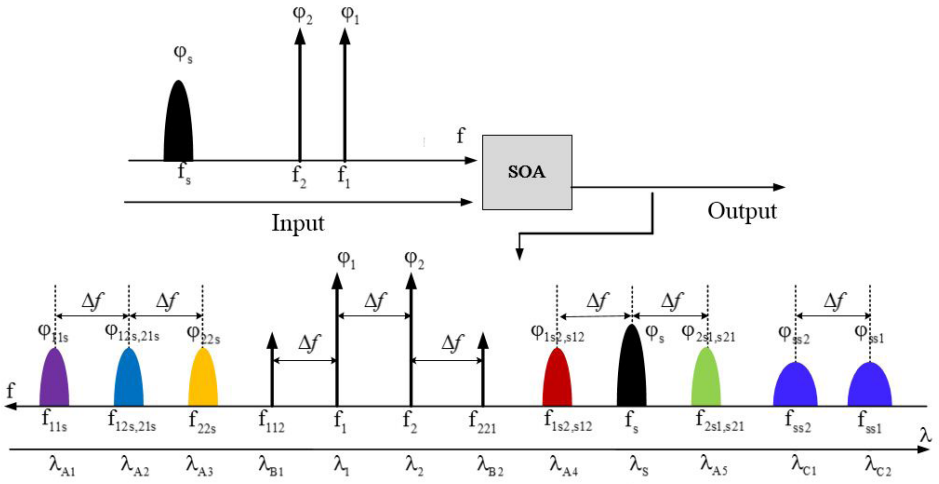

Fig. 1. Operation principle of wavelength multicasting scheme based on FWM in SOA.

For the generated idlers at λ_{B1} and λ_{B2}, there will be no information because of the absent participation of the original input QPSK signal in the FWM processes.

The frequency detuning between the pump and signal needs to be specified to avoid overlapping of the new generated idlers and reduce the cross talk between channels. The relationship of the frequency interval of the new generated idlers with the two pumps' frequency spacing is shown in Fig. 1. With two pumps, five new multicast channels will be achieved, to obtain more multicast channels, more pumps are preferred to generate more FWM components[21].

The experimental setup for the 25 Gb/s QPSK WDM wavelength multicasting in SOA is shown in Fig. 2. The light sources of the input QPSK signal, the pumps, and the local oscillator (LO) at the coherent receiver are all with narrow linewidth of 100 kHz in order to reduce the added phase noise. On the signal branch, the light from an external cavity laser (ECL) at 1552.52 nm (193.1 THz) is modulated by a single inphase/quadrature (IQ) modulator with 23 GHz 3 dB bandwidth and 5 V half-wave voltage. The IQ-modulator is driven by two de-correlated two level driving electronics provided by pseudo-random binary sequence (PRBS) streams which are generated by an arbitrary waveform generator (AWG). The length of the PRBS stream is $2^{15} - 1$. An erbium-doped fiber amplifier (EDFA) is used to amplify the signal and a 1 nm optical band-pass filter (OBPF) is employed to filter out the out-of-band noise. The polarization controller (PC) is placed along the path between the EDFA and OBPF to adjust the polarization of the signal light to optimize the FWM efficiency. On the pump branch, two pumps at 1549.32 nm (193.5 THz) and 1550.12 nm (193.4 THz) are generated by two tunable ECLs. Then combined with a WDM multiplexer (MUX) together with the generated NRZ-QPSK signal is injected into the SOA through a 3 dB coupler. The two pumps are set co-polarized with each other by properly adjusting the PCs to reduce the system polarization sensitivity[22,23]. The SOA (CIP SOA-NL-OEC-1550) being used here is a commercially available device operating over the C-band which has a small signal gain of 34 dB, 6 dBm saturation output power, and typical 0.5 dB polarization-dependent gain value. The carrier recovery time of the SOA is typically 25 ps which does not cause any degradation to the multicast signals. The measured power for each pump before the MUX is 6 dBm. The power of the signal light before the coupler is −4 dBm. The total power in and out of the SOA are 5.75 and 13.93 dBm, respectively. The bias current of the SOA is set as 280 mA. At the output of the SOA, the new generated FWM terms are filtered by a 1–9 Finisar wavelength selective switch (WSS) (Finisar DWPF, Flexgird) based on liquid crystals on silicon with variable bandwidth and then sent to a coherent receiver which includes a LO, an optical 90° hybrid, and two balanced photodetectors (BPDs) for detection and BER measurement. A variable optical attenuator (VOA) and EDFA will be used as pre-amplifier before the hybrid. After the BPDs, the data are sampled by a real-time storage oscilloscope operating at 80 GSa/s with 30 GHz electrical bandwidth (Tektronix MSO 73304DX). The captured data will be off-line processed through the digital signal processing method.

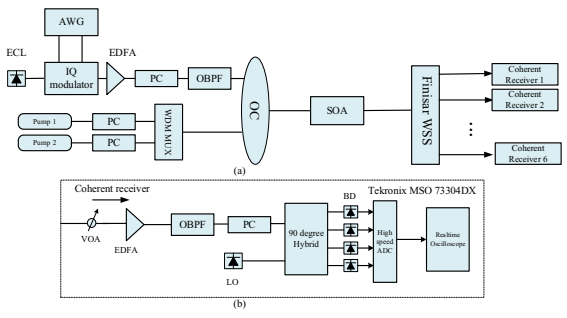

Fig. 2. Experimental setup of: (a) QPSK multicasting in SOA and (b) coherent receiver. OC, optical coupler; BD, balanced detector; ADC, analog-to-digital converter.

Figure 3 shows the spectra measured at the input and output of the SOA, the input NRZ-QPSK signal light and two pump lights are indicated by λ_s, and λ_1, and λ_2, respectively. At the output of the SOA, as analyzed above, five new generated idlers will preserve the information of the original QPSK signal, denoted by λ_{A1}–λ_{A5} in Fig. 3. The idlers at λ_{B1} and λ_{B2} carry no information. At λ_{C1} and λ_{C2}, two BPSK signals will be obtained. With our current experimental setup, by changing the frequency spacing between the signals and pumps, the output multicasting channels can be consistent with the ITU channels. Frequency detuning is another important factor that can influence the FWM CE. With a reasonable frequency detuning, a good CE can be achieved, whereas with too large frequency detuning, the CE will decrease obviously. In our experiment, the frequency detuning of f_1 to f_2 and f_2 to f_s are 100, and 300 GHz, respectively. With the current frequency detuning, acceptable CE was achieved.

Figure 4 shows the BER performance of the multicast QPSK channels (including the output signal at λ_s for reference) as a function of the received power, the

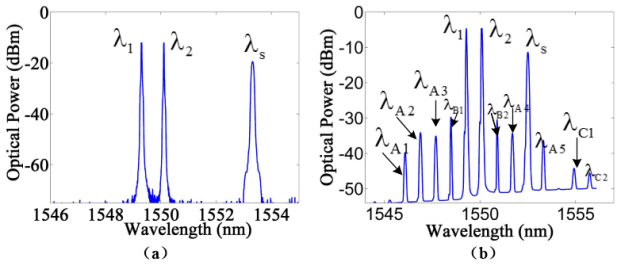

Fig. 3. Optical spectrum at the (a) input and (b) output of SOA.

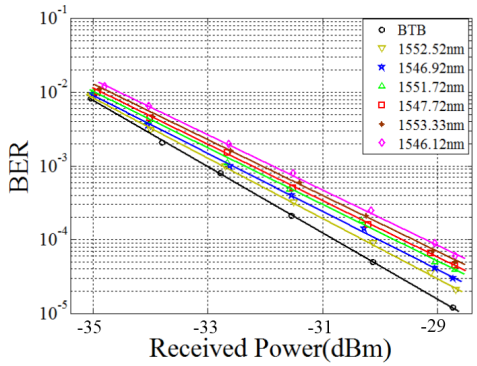

Fig. 4. Measured BER performance versus received power of the multicast channels.

back-to-back performance is also measured as a reference. From Fig. 4 we can see that the whole five multicast channels are all with low power penalties (from about 0.4 dB to less than 1.1 dB) at the BER of 10^{-3}, their detailed performances including the wavelength, CE (defined as the ratio of the converted signal power to that of the input signal power), and power penalty at a BER of 10^{-3} are summarized in Table 1.

From Table 1 it can be seen that the power penalty is sensitive to the CE which directly influences the OSNR of the converted signal. When the CE of the generated idlers at λ_{A2} and λ_{A4} is larger than −23 dB, the power penalty is less than 0.6 dB. On the other hand, the power penalty of the idlers at λ_{A1}, λ_{A3}, and λ_{A5} is larger than 0.7 dB because the CE is smaller than −23 dB. To further present the relationship between CE and input pump and signal powers in SOA, we give a characterization of CE using the BER as a figure of merit in the following.

Before the multicast signals were detected by the coherent receiver, we measured the spectra of the each wavelength at the output of the WSS, as shown in Fig. 5. The insets are the constellation and corresponding I and Q eye diagrams of the multicast QPSK signals after coherent detection and demodulation. The concentrated constellation and clear open eye proves the good quality of the multicast QPSK signal.

Figure 6(a) depicts the measured CE and BER as a function of the input signal power for the multicast channels at 1551.72 and 1546.12 nm when fixing the pump power at 6 dBm. It is obvious that the CE almost does not benefit from the increasing signal power, but when signal power is increasing it does help to drop the BER. However, when further increasing the signal power larger than −4 dBm, the increasing BER is obvious which is probably caused by the self-phase modulation introduced distortions. On the other hand, as Fig. 6(b) shows, when increasing the pump power it does make contribution to the CE. With a good CE, a sufficient OSNR will be obtained therefore resulting in a good BER performance. However, when the pump power is larger than 6 dBm, the added noise from cross-phase modulation (XPM) effects will distort the performance resulting in increasing BER. As discussed in Refs. [24, 25], the limited OSNR of the pump light will intensify the XPM effect resulting in a more severe performance degradation. Additionally, in-band cross talk due to high-order FWM, products can be particularly critical when the pump power is larger than 8 dBm. Figure 6 shows that not always with a high CE there will be a good BER performance but rather a compromise between the CE and the nonlinear noise. So, to eliminate the deleterious components in the converted signal, the powers of the pumps and signals should be optimized. In our experiment, the optimal powers of the pump and signal are 6 and −4 dBm, respectively. The average CE of the five new generated QPSK channels is −24.12 dB when the BER is the best. In our experiment, the two pumps are set to be co-polarized with each other and parallel to the signal to maximize the FWM efficiency. Not all of the generated idlers from λ_{A1} to λ_{A5} will be polarization independent with the input signal, only λ_{A4} and λ_{A5} will be polarization insensitive. And when adjusting the polarization of the signal parallel to the pumps, a best FWM efficiency will be obtained for all the five channels. Orthogonal pumps scheme[22] and polarization diversity scheme with two independent circuits[26] can also be considered to reduce the polarization sensitivity.

In conclusion, we discuss a NRZ-QPSK wavelength multicasting based on FWM process in SOA. We experimentally demonstrate the one-to-five 25 Gb/s NRZ-QPSK signal WDM multicasting employing two pumps. The

Table 1. Multicast Channel Performance

	Wavelength (nm)	**Estimated OSNR (dB)**	**CE (dB)**	**Power Penalty (dB)**
λ_{A1}	1546.12	16.1	−28	1.1
λ_{A2}	1546.92	21	−22.4	0.4
λ_{A3}	1547.72	18.7	−23.4	0.7
λ_{A4}	1551.72	19.5	−22.8	0.6
λ_{A5}	1553.33	16.8	−24	0.82

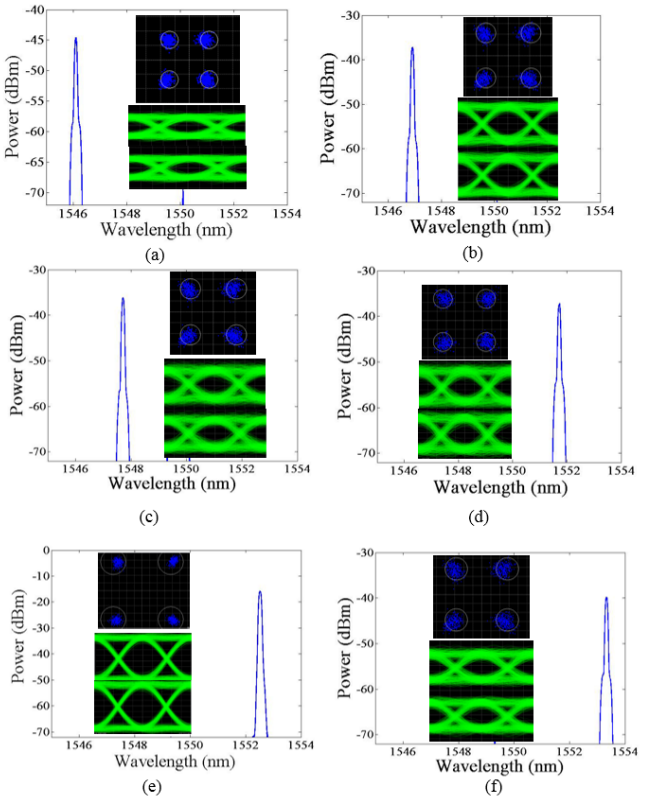

Fig. 5. Optical spectra of the multicast QPSK channels after the WSS at different wavelengths: (a) λ_{A1}, 1546.12 nm, (b) λ_{A2}, 1546.92 nm, (c) λ_{A3}, 1547.72 nm, (d) λ_{A4}, 1551.72 nm, (e) λ_s, 1552.52 nm, and (f) λ_{A5}, 1553.33 nm. Insets: constellation and I/Q eye diagrams of the multicast signal on each wavelength.

multicast channels are all compliant with the ITU grid. All the new generated QPSK channels are with a power penalty less than 1.1 dB at a BER of 10^{-3} and their respective constellation and eye diagram are presented. We also give a characterization of the CE in terms of input signal and pump powers using the BER as a figure of merit, the results indicate that the pump and signal powers need to be carefully controlled to avoid the performance distortion introduced by nonlinear effects. The SOA can be useful for WDM multicasting in the optical network for its integration potential, low power consumption, and high CE.

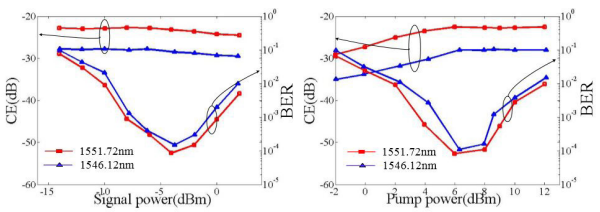

Fig. 6. Measured CE and BER when (a) tuning input signal power with fixed pump power and (b) tuning input pump power with fixed signal power.

This work was supported by the National 863 Program of China under Grant Nos. 2012AA011302 and 2011AA010306.

References

1. G. N. Rouskas, IEEE Netw. **17,** 60 (2003).
2. K. Inoue, T. Hasegawa, K. Oda, and H. Toba, Electron. Lett. **29,** 1708 (1993).
3. G. W. Lu, K. S. Abedin, and T. Miyazaki, Opt. Express **16,** 21964 (2008).
4. C. S. Bres, A. Wiberg, B. P. Kuo, N. Alic, and S. Radic, IEEE Photon. Technol. Lett. **21,** 1002 (2009).
5. O. F. Yilmaz, S. R. Nuccio, X. Wang, J. Wang, I. Fazal, J. Y. Yang, X. Wu, and A. E. Willner, in *Proceedings of Optical Fiber Communication Conference* 1 (2010).
6. Z. Chen, L. Yan, W. Pan, B. Luo, A. Yi, Y. Guo, and J. Lee, IEEE Photon. Technol. Lett. **24,** 1882 (2012).
7. R. Adams, M. Spasojevic, M. Chagnon, M. Malekiha, J. Li, D. Plant, and L. Chen, in *Proceedings of IEEE Photonics Conference (IPC)* 1 (2013).
8. M. Pu, H. Hu, H. Ji, M. Galili, L. K. Oxenlowe, P. Jeppesen, J. M. Hvam, and K. Yvind, Opt. Express **19,** 2448 (2011).
9. A. Malacarne, G. Meloni, G. Berrettini, N. Sambo, L. Poti, and A. Bogoni, J. Lightwave Technol. **31,** 1797 (2013).
10. A. Mecozzi, S. Scotti, A. D'ottavi, E. Iannone, and P. Spano, J. Quant. Electron. **31,** 689 (1995).
11. G. Contestabile, M. Presi, and E. Ciaramella, IEEE Photon. Technol. Lett. **16,** 1775 (2004).
12. B. Filion, W. Ng, A. T. Nguyen, L. A. Rusch, and S. LaRochelle, Opt. Express **21,** 19825 (2013).
13. S. Gao, E. K. Tien, Y. Huang, and S. He, Opt. Express **18,** 27885 (2010).
14. G. Contestabile, A. Maruta, S. Sekiguchi, K. Morito, M. Sugawara, and K. Kitayama, J. Quant. Electron. **47,** 541 (2011).
15. G. Contestabile, Y. Yoshida, A. Maruta, and K. Kitayama, Opt. Express **20,** 27902 (2012).
16. G. Contestabile, A. Maruta, and K. I. Kitayama, J. Quant. Electron. **50,** 379 (2014).
17. J. Hansryd, P. A. Andrekson, M. Westlund, J. Li, and P. O. Hedekvist, IEEE J. Sel. Top. Quant. Electron. **8,** 506 (2002).
18. N. Deng, K. Chan, C. K. Chan, and L. K. Chen, IEEE J. Sel. Top. Quant. Electron. **12,** 702 (2006).
19. G. W. Lu, K. S. Abedin, and T. Miyazaki, J. Lightwave Technol. **27,** 409 (2009).
20. G. W. Lu, E. Tipsuwannakul, T. Miyazaki, C. Lundstrom, M. Karlsson, and P. A. Andrekson, J. Lightwave Technol. **29,** 2460 (2011).
21. Y. Chen, J. Li, P. Zhu, B. Guo, L. Zhu, Y. He, and Z. Chen, Opt. Express **21,** 9915 (2013).
22. G. Contestabile, L. Banchi, M. Presi, and E. Ciaramella, J. Lightwave Technol. **27,** 4256 (2009).
23. J. Ma, J. Yu, C. Yu, Z. Jia, X. Sang, Z. Zhou, T. Wang, and G. K. Chang, J. Lightwave Technol. **24,** 2851 (2006).
24. R. Elschner and K. Petermann, in *LEOS Annual Meeting Conference Proceedings, 2009. LEOS'09. IEEE* 779 (2009).
25. G. W. Lu, T. Sakamoto, and T. Kawanishi, Opt. Express **22,** 15 (2014).
26. G. Contestabile, A. D'Ottavi, F. Martelli, P. Spano, and J. Eckner, IEEE Photon. Technol. Lett. **14,** 666 (2002).